Effects of C2 hemisection on respiratory and cardiovascular functions in rats

Pauline Michel-Flutot, Arnaud Mansart, Abdallah Fayssoil, Stéphane Vinit

NEURAL REGENERATION RESEARCH
www.nrronline.org

Research Article

Effects of C2 hemisection on respiratory and cardiovascular functions in rats

Pauline Michel-Flutot[1], Arnaud Mansart[2], Abdallah Fayssoil[1, 3], Stéphane Vinit[1, *]

https://doi.org/10.4103/1673-5374.346469

Date of submission: January 3, 2022

Date of decision: March 14, 2022

Date of acceptance: April 22, 2022

Date of web publication: June 2, 2022

From the Contents

Graphical Abstract

A C2 spinal cord lateral hemisection induces a diaphragm hemiplegia and a systolic dysfunction in rats at 7 days post-injury

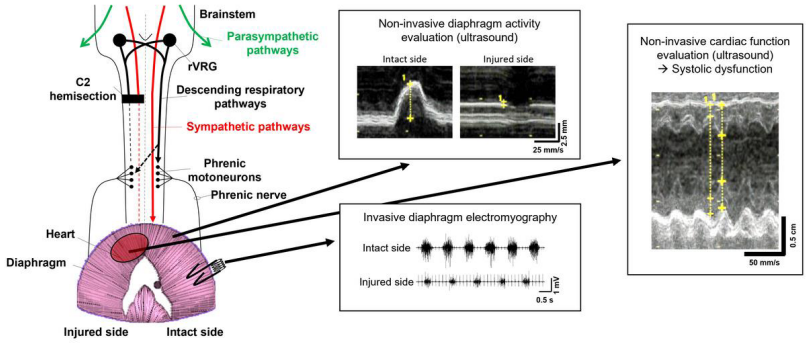

Abstract

High cervical spinal cord injuries induce permanent neuromotor and autonomic deficits. These injuries impact both central respiratory and cardiovascular functions through modulation of the sympathetic nervous system. So far, cardiovascular studies have focused on models of complete contusion or transection at the lower cervical and thoracic levels and diaphragm activity evaluations using invasive methods. The present study aimed to evaluate the impact of C2 hemisection on different parameters representing vital functions (i.e., respiratory function, cardiovascular, and renal filtration parameters) at the moment of injury and 7 days post-injury in rats. No ventilatory parameters evaluated by plethysmography were impacted during quiet breathing after 7 days post-injury, whereas permanent diaphragm hemiplegia was observed by ultrasound and confirmed by diaphragmatic electromyography in anesthetized rats. Interestingly, the mean arterial pressure was reduced immediately after C2 hemisection, with complete compensation at 7 days post-injury. Renal filtration was unaffected at 7 days post-injury; however, remnant systolic dysfunction characterized by a reduced left ventricular ejection fraction persisted at 7 days post-injury. Taken together, these results demonstrated that following C2 hemisection, diaphragm activity and systolic function are impacted up to 7 days post-injury, whereas the respiratory and cardiovascular systems display vast adaptation to maintain ventilatory parameters and blood pressure homeostasis, with the latter likely sustained by the remaining descending sympathetic inputs spared by the initial injury. A better broad characterization of the physiopathology of high cervical spinal cord injuries covering a longer time period post-injury could be beneficial for understanding evaluations of putative therapeutics to further increase cardiorespiratory recovery.

Key Words: C2 spinal cord injury; cardiovascular; diaphragm activity; heart function; hemiplegia; rat model; respiratory; ultrasound

Introduction

High cervical spinal cord injuries (SCI) induce permanent neuromotor and autonomic deficits in vital functions, such as respiratory, cardiovascular, and renal functions (Eckert and Martin, 2017). People living with high SCI are frequently mechanically ventilated and often present cardiac dysfunction (Ahuja et al., 2017; Eli et al., 2021). However, compensatory mechanisms can occur spontaneously to allow the survival of these patients and some functional recovery (Chay and Kirshblum, 2020). To study the pathophysiological processes and subsequent compensatory mechanisms following a high cervical injury, a reliable preclinical animal model is required since human studies are limited. Among preclinical models of high SCI, the rat C2 hemisection (C2HS) model is the most documented, and this injury impacts both the central respiratory and cardiovascular systems (Keomani et al., 2014; Navarrete-Opazo et al., 2015; Vinit et al., 2016; Bezdudnaya et al., 2018; Cheng et al., 2021a; Jesus et al., 2021; Michel-Flutot et al., 2021, 2022; Rana et al., 2021).

In the central nervous system, the descending respiratory pathway originates from the rostral ventral respiratory group and is located in the rostro-ventral medulla (Feldman et al., 2013). It bilaterally and monosynaptically connects to the phrenic motoneuron pool (at the C3–C6 spinal segments of the spinal cord) that bilaterally innervates the diaphragm (which is the main inspiratory muscle) via the phrenic nerve (Feldman et al., 1985; Lipski et al., 1986; Vandeweerd et al., 2018). Lateral hemisection at the C2 spinal cord segment induces deafferentation of the corresponding phrenic motoneuron pool below the lesion, leading to immediate hemidiaphragm paralysis (Vinit et al., 2006). With this injury, the presence of a contralateral intact spinal cord allows animal survival (Fuller et al., 2008; Keomani et al., 2014; Bezdudnaya et al., 2018; Cheng et al., 2021a; Rana et al., 2021). In this model, modest respiratory recovery can be observed on the injured side and is mainly sustained by silent pathways connected to the deafferented phrenic motoneurons that cross the spinal cord midline at the C3–C6 level. This recovery is termed the crossed phrenic phenomenon (Goshgarian, 2003; Fuller et al., 2008; Vinit and Kastner, 2009; Ghali, 2017; Bezdudnaya et al., 2018). C2HS also induces the loss of half of the descending vasomotor axons that innervate the cardiovascular system. Anatomically, sympathetic regulation of the heart and vessels arises from the metameric thoracic T1-L2 spinal cord levels (Hou and Rabchevsky, 2014). Parasympathetic regulation originates from the brainstem and sends information through the vagus and glossopharyngeal nerves (Hou and Rabchevsky, 2014). In upper spinal cord injury, following the cervical injury, the parasympathetic activities remain intact and will overcome the sympathetic influence, producing a *de facto* impact on sympathetic/parasympathetic homeostasis and causing autonomic dysfunction, including cardiovascular dysregulation and renal function alteration (Hou and Rabchevsky, 2014; Biering-Sørensen et al., 2018). In humans living with chronic high SCI, orthostatic hypotension with episodes of

[1]Université Paris-Saclay, UVSQ, Inserm, END-ICAP, Versailles, France; [2]Université Paris-Saclay, UVSQ, Inserm, Infection et Inflammation (2I), Versailles, France; [3]Raymond Poincaré Hospital, AP-HP, Garches, France

***Correspondence to:** Stéphane Vinit, PhD, HDR, stephane.vinit@uvsq.fr.

https://orcid.org/0000-0001-7013-1741 (Stéphane Vinit)

Funding: *This work was supported by funding from the Chancellerie des Universités de Paris (Legs Poix) (to SV), Fondation Medisite (to SV), INSERM (to SV, AM, AF) and Université de Versailles Saint-Quentin-en-Yvelines (to SV, AM, AF).*

How to cite this article: *Michel-Flutot P, Mansart A, Fayssoil A, Vinit S (2023) Effects of C2 hemisection on respiratory and cardiovascular functions in rats. Neural Regen Res 18(2): 428-433.*

autonomic dysreflexia (high arterial hypertension induced by either noxious or non-noxious stimuli) is often observed (Krassioukov and Claydon, 2006). In addition, left ventricular remodeling affecting the lower left ventricular (LV) mass, increasing the LV wall thickness, or worsening LV diastolic function can also be observed (Kessler et al., 1986; Driussi et al., 2014), again depending on the level and extent of injury (West et al., 2012). On top of this, a meta-analysis bringing together more than 80,000 outpatients and inpatients presenting heart failure, showed that more than 60% of these patients also displayed kidney failure (Smith et al., 2006). This makes the evaluation of the renal function of interest following high SCI. However, cardiovascular outcomes following acute high cervical SCI have not yet been well investigated.

Immediately following SCI, patients experience life-threatening conditions (Eli et al., 2021). The recommended initial treatment is to immobilize and stabilize the patient, maintaining the mean arterial pressure (MAP) between 85–90 mmHg (Eli et al., 2021). Functional research evaluations in acute SCI stages are consequently impossible in humans. Therefore, preclinical models are necessary to understand the cardiovascular physiopathology following acute and subacute SCI stages, but unfortunately, no data are available from preclinical models of high cervical spinal cord injury. Transection or contusion of the rat spinal cord at the thoracic level on rats to facilitate evaluations of associated cardiovascular dysfunction is common (Weaver et al., 1997; Squair et al., 2017, 2018a). These models display an increased heart rate and sympathetic tonus and decreased MAP (Lujan et al., 2018) associated with cardiac atrophy and contractile dysfunction 12 weeks post-injury (Poormasjedi-Meibod et al., 2019). Nevertheless, few studies have used lower-cervical models of SCI, and these studies always applied complete transection, with bradycardia, hypotension, and a reduced heart rate and sympathetic tonus observed weeks after injury (Lujan et al., 2018; Lujan and DiCarlo, 2020). These diverse preclinical studies used invasive and terminal experiments to assess the pathophysiology of respiratory insufficiency (i.e., diaphragm electromyography (Vinit et al., 2006; Terada and Mitchell, 2011; Keomani et al., 2014; Warren et al., 2018)) and cardiovascular dysregulation (telemetry (Mayorov et al., 2001) and terminal arterial pressure recordings (Bravo et al., 2002)) following SCI.

Ultrasound is a non-invasive and reliable clinical method to study moving organs such as the diaphragm (Fayssoil et al., 2018) and heart (Papadimitriou et al., 2016; Shimron et al., 2018) under several pathologies, including in patients living with SCI (Ditterline et al., 2020; Zhu et al., 2021). A few preclinical animal studies have used ultrasound to evaluate diaphragm activity in intact animals (Ioannis et al., 2016; Fayssoil et al., 2021), but none have evaluated diaphragmatic dysfunction following cervical SCI. However, this technique is commonly used to evaluate cardiac function in intact rats (Pacher et al., 2008; Harman et al., 2018) and even following thoracic SCI (DeVeau et al., 2018; Squair et al., 2018a, b). Although no studies have evaluated the cardiovascular effect of incomplete cervical SCI in a preclinical animal model, most patients living with SCI suffer from high-level (cervical) and often incomplete spinal injury.

In the present study, we investigated several vital physiological parameters (respiratory function, cardiovascular function, and renal filtration) 7 days post-C2 spinal cord hemisection in Sprague-Dawley rats.

Methods

Ethics statement

All experiments reported in this manuscript conformed to policies set by the National Institutes of Health (USA) in the Guide for the Care and Use of Laboratory Animals and EU Directive 2010/63/EU for animal experiments. These experiments were performed on 44 male Sprague-Dawley rats (7-week-old, body weight 350 g, Janvier, Le Genest-Saint-Isle, France). We did not use female rats to avoid non-reproductible data due to hormonal cycle. Hormonal cycle change is linked to respiratory changes (Behan and Kinkead, 2011). The animals were dual-housed in individually ventilated cages in a state-of-the-art animal care facility (2CARE animal facility, accreditation A78-322-3, France) with access to food and water *ad libitum* and a 12-hour light/dark cycle. These experiments were approved by the Ethics Committee of the University of Versailles Saint-Quentin-en-Yvelines and complied with French and European laws regarding animal experimentation (Apafis #2017111516297308, approval date August 9, 2021). The experimental design is provided in **Figure 1** for a better clarity in the experimental design.

Chronic C2 spinal cord hemisection

Before anesthesia, the rats were subcutaneously injected with the pre-anesthetic drugs buprenorphine (0.03 mg/kg; Buprécare, Axience, Pantin, France), trimethoprim and sulfadoxin (Borgal 24%, 30 mg/kg; Virbac, Carros, France), medetomidine (0.1 mg/kg; Médétor, Virbac), and carprofen (Rimadyl, Zoetis, Malakoff, France, 5 mg/kg). Approximately 10 minutes after injection, anesthesia was induced in a closed chamber (5% isoflurane in 100% O_2). The rats were then intubated and ventilated with a rodent ventilator (model 683; Harvard Apparatus, South Natick, MA, USA), and anesthesia was maintained with isoflurane (2.5% in 100% O_2) throughout the surgical procedure. After the skin and muscles were retracted, laminectomy and durotomy were performed at the C2 level. The spinal cord was then sectioned unilaterally (left side) with microscissors. A microscalpel was used immediately after the microscissors to ensure the existence of a potential section of remaining fibers as previously described (Keomani et al., 2014). The muscles and skin

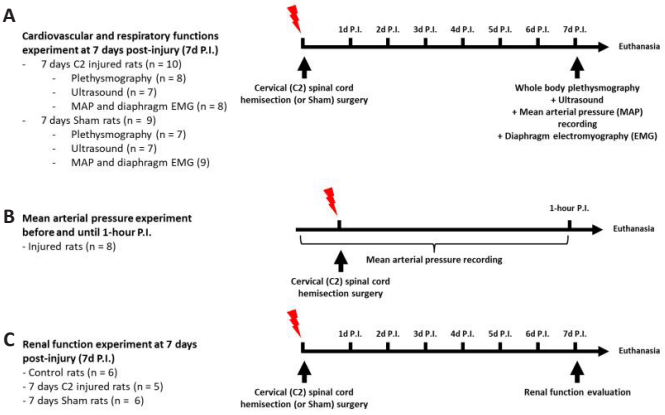

Figure 1 | **Experimental design.**
(A) Timeline for experiments done at 7 days (7 d) following surgery for injured and sham animals, i.e., whole body plethysmography, ultrasound, mean arterial pressure (MAP) recording and diaphragm electromyography (EMG) recording. (B) Timeline for experiments done before and until 1-hour post-injury (PI) for mean arterial pressure recording. (C) Timeline for experiments done at 7 d PI for renal function evaluation.

were then sutured. To reverse the effect of medetomidine, atipamezole (0.5 mg/kg; Revertor, Virbac) was intramuscularly injected. The isoflurane anesthesia was then turned off, and when the rats showed signs of waking up, the endotracheal tube was removed. Sham rats received the same surgery without C2 spinal cord hemisection. In this study, a total of 18 rats received a C2 spinal cord hemisection, and a total of 9 rats received a sham surgery.

Whole-body plethysmography

In total, 15 rats were used for whole-body plethysmography recordings. The rats were randomly divided into two groups: sham (n = 7) and 7 days post-injury (7 d PI, n = 8).

Whole-body constant flow (2 L/min) plethysmography (EMKA, France) was used to assess global ventilatory function (e.g., the tidal volume, minute ventilation, and breathing frequency) in our rats, as previously described (Fayssoil et al., 2021). The rats were weighed, and the plethysmography system was calibrated before the animals were placed in the chambers. After a 30-minute acclimation period, recording began under normoxic conditions (room air). The minute ventilation and tidal volume were reported according to the bodyweight (per 100 g) for each animal. Data obtained from one of the sham rats were corrupted and therefore could not be analyzed, meaning the number of plethysmography recordings used for this group is n = 6.

Echography data acquisition

In total, 14 from the 15 rats used for whole-body plethysmography recordings were also used for ultrasound data acquisition. The rats were randomly divided into two different groups: sham (n = 7) and 7 d PI (n = 7). One of the rats from the 7 d PI group used for whole-body plethysmography recordings was not used for ultrasound recordings due to technical event.

To evaluate diaphragm activity and cardiac function, a high-resolution ultrasound system (LOGIQ E9; GE, Solingen, Germany) and a high-frequency (18 MHz) linear L8-18i probe (GE) were used. Anesthesia was induced by isoflurane (5% at 500 mL/min in 100% O_2) in a closed chamber and maintained through a nose cone (isoflurane balanced at 1.5–2% in 100% O_2). Each rat's anterior thorax and upper abdomen were shaved before exploration. The rats were placed in the supine position on the imaging platform, and their rectal temperature was monitored and maintained at 37.5 ± 0.5°C throughout the experiment. Ultrasound gel was applied to the chest skin before measurement.

After visualization of the diaphragm, M-mode ultrasound was used to assess the diaphragm motion (diaphragmatic inspiratory motion (**Figure 2**), and inspiratory time and expiratory time (**Table 1**)) from the subcostal view (Fayssoil et al., 2021).

Table 1 | **Whole body plethysmography in unanesthetized eupneic rats**

	Mean ± SD (minimum–maximum)	
Parameters	**7 d Sham**	**7 d PI**
T_I (ms)	186 ± 26 (161–230)	208 ± 34 (163–279)
T_E (ms)	350 ± 77 (266–448)	307 ± 53 (215–392)
V_M (mL/min/100 g)	43.80 ± 7.00 (35.83–54.19)	42.02 ± 6.71 (31.65–53.23)
V_T (mL/100 g)	0.37 ± 0.03 (0.32–0.40)	0.34 ± 0.03 (0.29–0.37)
Respiratory rate (breaths/min)	120 ± 17 (102–146)	125 ± 20 (92–159)

PI: Post-injury; T_E: expiratory time; T_I: inspiratory time; V_M: minute ventilation; V_T: tidal volume. 7 d Sham (n = 6) and 7 d PI (n = 8).

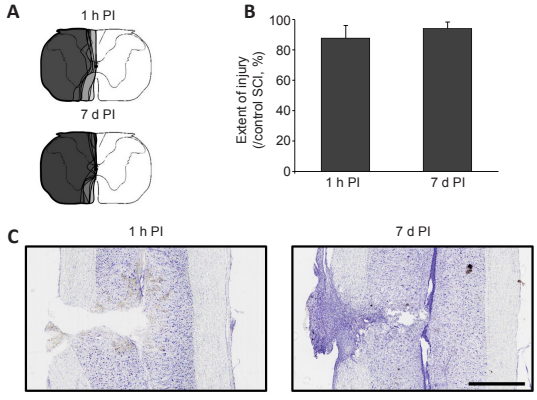

Figure 2 | **Extent of injury following a C2 spinal cord hemisection.**
(A) Representative extend of injury in each animal at 1 hour post-injury (1 h PI) (n = 8), and 7 days (7 d) PI (n = 10). The representative extent of injury has been superimposed for each group. (B) Extent of injury quantification in percentage compared to control, i.e., total spinal cord hemisection (100%). There was no difference between the two groups (Student's t-test, P = 0.070). (C) Representative longitudinal spinal cord cross sections stained with cresyl violet for the 1 h PI and 7 d PI groups. Pictures display the site of injury. The C2 hemisection was clearly visible at 1 h PI, whereas a scar was observed at the site of injury by 7 days PI. Scale bar: 1 mm. PI: Post-injury.

2D-mode ultrasound was used to measure the diaphragm thickness and assess thickening from the apposition zone during live breathing, as previously described (Fayssoil et al., 2021). For this assessment, the probe was placed perpendicularly to the chest wall at the midaxillary line to visualize the costophrenic sinus. In the apposition zone, clear visualization of the diaphragm can be recorded, as bounded by 2 clear bright lines—the pleural line and the peritoneal line. The thicknesses of the diaphragm at the end of the expiration and inspiration cycles were also recorded. The thickening fraction of the diaphragm was calculated using the following ratio: (thickness at end inspiration–thickness at end expiration)/thickness at end expiration (Matamis et al., 2013; Fayssoil et al., 2021).

For echocardiographic recording, the sweep speed, depth, focus, and gain settings were optimized to obtain the best images. The LV diastolic and systolic diameters were measured from an M-mode short-axis view of the left ventricle at the papillary muscle level. The LV ejection fraction was calculated from the M-mode measurements. The aortic velocity time integral was recorded by Doppler echocardiography during the procedure. The mitral inflow Doppler pattern was recorded (peak E, peak A (used to calculate the E/A ratio), and deceleration time) from a 4-chamber apical view.

Electrophysiological and hemodynamic recordings

All animals used for the echography experiments were also used for diaphragm electromyographic recordings, except one animal in the 7 d PI group that died after the ultrasound experiment: sham (n = 7) and 7 d PI (n = 6).

In total, 25 rats were used for MAP recordings. The rats were randomly divided into three different groups: Before injury (n = 8), in which the rats underwent C2 spinal cord hemisection during recording and were kept until 1 hour PI; 7 d sham (n = 9) and 7 d PI (n = 8). All animals used for diaphragm electromyographic recordings were also used for hemodynamic recordings and were therefore included in the corresponding groups.

As previously described (Keomani et al., 2014), anesthesia was induced using isoflurane (5% balanced in 100% O_2) in an anesthesia chamber and then maintained through a nose cone (2.5% balanced in 21% O_2). The rats were placed on a heating pad, and the rectal temperature was continuously monitored throughout the experiment (maintained at 37.5 ± 0.5°C). A catheter was inserted in the right femoral artery to measure the arterial pressure and heart rate. The arterial and tracheal pressures were monitored continuously by transducers connected to a bridge amplifier (AD Instruments, Dunedin, New Zealand). The appropriate depth of anesthesia was confirmed by the absence of any response to toe pinching. The arterial pressure and heart rate were recorded for at least 10 minutes. Then, a laparotomy was performed, and the liver was gently moved caudally to access the diaphragm. To prevent dehydration, gauze soaked with warm phosphate-buffered saline was placed on the liver. A handmade bipolar-surface silver electrode connected to an amplifier (Microelectrode AC amplifier Model 1800; A-M SYSTEMS, Sequim, WA, USA) was used to record diaphragm electromyographic activity (EMGdia). The electrode was gently placed on the crural part of each hemidiaphragm during spontaneous poïkilocapnic normoxic breathing as previously described (Keomani et al., 2014; Vinit et al., 2016). The recorded signals were digitized by an 8-channel Powerlab data acquisition device (Acquisition rate: 100 k/s; AD Instruments, Dunedin) connected to a computer and analyzed using LabChart 8 Pro software (AD Instruments, Dunedin).

Renal function evaluation

Renal function was evaluated in 17 rats by determining the glomerular filtration rate (GFR) and renal threshold for glucose excretion. The rats were randomly divided into three groups: control (n = 6), 7 d sham (n = 6), and 7 d PI (n = 5). The animals were anesthetized by intraperitoneal injection of ketamine (100 mg/kg; Kétamine, Virbac) + xylazine (10 mg/kg; Rompun, Bayer, La Garenne-Colombes, France) and then placed in the supine position. The body temperature was continuously monitored using a rectal probe and maintained at 37.5 ± 0.5°C. After a laparotomy, a catheter was inserted into the bladder for urine collection. Two additional catheters were inserted, with 1) one placed into the right jugular vein for intravenous injection of inulin solution (inulin 10 mg/kg + mannitol 1 g/kg bodyweight at 0.1 mL/min) and 2) one placed into the left carotid artery for blood sampling. After an acclimation period of 10 minutes, inulin solution was injected (0.1 mL/min at 37°C) for 20 minutes. Urine output was collected during the last 10 minutes of inulin injection. Afterward, 250 µL of blood was collected from the arterial catheter. The inulin concentration in plasma and urine samples was determined by the anthrone method (Moreira et al., 2014). A second solution was then injected to determine the renal threshold for glucose, which was a perfusion of glucose (0.8 g/kg) + mannitol (1 g/kg) at 0.1 mL/min for 20 minutes. Urine and blood were collected as described above. The relationship between urinary glucose excretion (UGE) and blood glucose (BG) is commonly described as a threshold relationship in which UGE is low (BG < renal threshold for glucose (RTG)), and UGE increases with the filtered glucose load when BG > RTG. In this case, the filtered glucose load is equal to the BG concentration multiplied by the GFR. This relation can be written mathematically as follows: rate of UGE (mg/min) = GFR (dL/min) × (BG (mg/dL) – RTG (mg/dL)). The RTG values were determined by nonlinear regression using previously measured BG and UGE values (Liang et al., 2012). The water reabsorption (%) was calculated as follows: (GFR (mL/min) – urine output (mL/min))/GFR (mL/min).

Tissue processing

At the end of the experiments, animals were euthanized by intracardiac injection of pentobarbital (EXAGON, Axience, Pantin, France, 0.2 mL/kg), intracardially perfused with heparinized 0.9% NaCl (10 mL) followed by Antigenfix solution (DIAPATH, Martinengo (BG), Italy). After perfusion, the C1–C3 spinal cord was carefully dissected and stored at 4°C in fixative for 24 hours. After post-fixation, tissues were cryoprotected for 48 hours in 30% sucrose (in 0.9% NaCl), and stored at –80°C. Frozen longitudinal C1–C3 spinal cord free floating sections (30 µm) were cut using a cryostat (NX70, Thermo Fisher Scientific, Waltham, MA, USA). Every fifth section was used for lesion reconstruction to examine the extent of C2 injury.

Histological reconstruction of the extent of C2 injury

Longitudinal sections from C1–C3 spinal cord were used to assess the dorso-ventral and medio-lateral extent of injury in all animals. Brightfield microscopy (Aperio AT2, Leica, Nanterre, France) was used to examine the sections stained with cresyl violet histochemistry (**Figure 2C**): 10 minute in cresyl violet solution (0.001% cresyl violet acetate (C5042-10G, Sigma-Aldrich, Darmstadt, Germany) and 0.125% glacial acetic acid (A/0400/PB15, Fisher Scientific, Illkirch, France) in distilled water), 1 minute in 70% ethanol, 1 minute in 95% ethanol, 2× 1 minute in 100% ethanol (E/0600DF/17, Fisher Scientific) and 2 minutes in xylene (X/0100/PB17, Fisher Scientific). They were then recorded on a stereotaxic transverse plane of the C2 spinal cord. Each injury was then digitized and analyzed with ImageJ 1.53n software (National Institutes of Health, Bethesda, MD, USA; Schneider et al., 2012). The extent of the injury on the injured side was calculated using a reference to a complete hemisection (which is 100% of the hemicord) and reported as a percentage as we published previously (Keomani et al., 2014).

Data processing

The amplitudes of the EMGdia recordings were double-integrated (Time Constant Decay = 50 ms) to maximally reduce the heartbeat signal interference. The average of at least 10 diaphragm contractions was calculated with LabChart 8 Pro software (AD Instruments, Dunedin).

Normality was tested with Shapiro-Wilk test. A paired t-test was performed to compare values between the intact and injured sides of the same animal (7 d PI) for inspiratory course and EMGdia analyses. The difference between two groups was assessed with two-tailed unpaired Student's t-test or with the non-parametric Mann-Whitney U test to compare the plethysmography analysis results between the 7 d sham and 7 d PI groups. Similar analysis was done for aortic diameters, and isovolumetric relaxation times. One-way analysis of variance was used to compare the results of the renal function evaluation and MAP experiments between different groups (control, 1 h PI, 7 d sham, and 7 d PI). One-way repeated-measures analysis of variance was used to compare the MAP and heart rate analysis results obtained from the same animal over time (before injury, 20 s PI and 1 h PI).

All data are presented as the mean ± SD, and values were considered significant when P < 0.05. For scatter plot analysis, confidence ellipses were calculated using the Khi2 confidence interval (95%). SigmaPlot 12.5 software (Systat Software, San Jose, CA, USA), and XLSTAT Premium 2016.1.1 (Addinsoft, Paris, France; https://www.xlstat.com) were used for all statistical analyses.

Results

Effects of C2 spinal cord hemisection on diaphragm activity

No difference in injury size between the 1 h PI (87.6 ± 8.5%) and 7 d PI (93.1 ± 4.6%) groups (P = 0.070) was observed (**Figure 2A–C**).

The plethysmography assessment of global ventilation showed no differences in the inspiratory time, expiratory time, minute ventilation, tidal volume, and respiratory rate between the 7 d sham and 7 d PI groups (**Table 1**).

A deeper diaphragm activity evaluation was also performed, in which the activity was first assessed non-invasively by ultrasound through inspiratory course evaluation (during diaphragm contraction) (**Figure 3A** and **B**). At 7 d PI, the intact side presented a similar inspiratory course to that of the 7 d sham group (P = 0.708), and a significantly higher value compared to the injured side (P < 0.001) (**Figure 3C**). Diaphragm activity was invasively evaluated in the same animals by diaphragm electromyography reflecting the neural drive to the diaphragm (**Figure 3D**). Similar to the inspiratory course, the integrated diaphragm amplitude in the intact side (7 d PI group) showed no difference compared to the 7 d sham group (P = 0.081) but was significantly higher than that in the injured side (P < 0.001) (**Figure 3E**). The relationship between the inspiratory course and integrated diaphragm amplitude was then explored. A positive relationship was observed, and the injured side of rats in the 7 d PI group was significantly different compared to rats in the 7 d sham group and the intact side of rats in the 7 d PI group (**Figure 3F**). Confidence ellipses were calculated using the Khi2 confidence interval (95%).

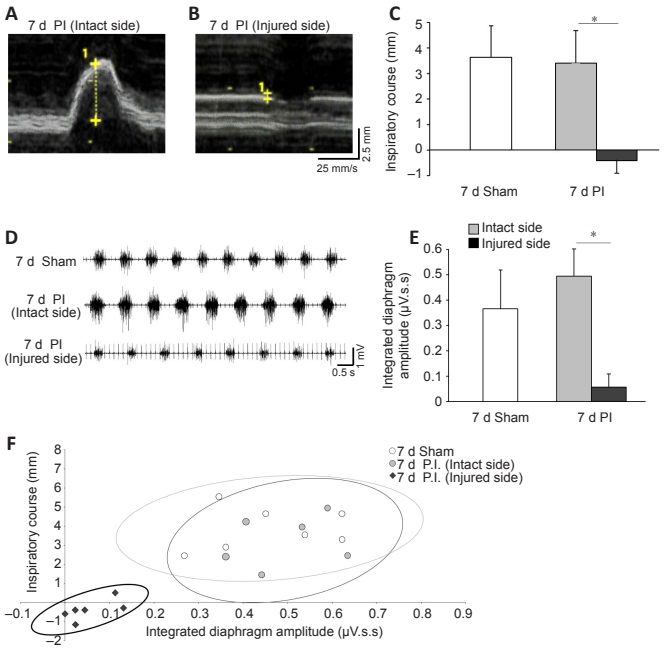

Figure 3 | **Evaluation of diaphragm activity following C2 spinal cord hemisection.** Representative traces of diaphragm contraction (inspiratory course) evaluated by ultrasound in anesthetized rats for intact side (A) and injured side (B). The scale bar in yellow was used to measure the inspiratory course values. (C) Quantification of inspiratory course measured by ultrasound in rats in the sham (n = 7) and 7 d PI groups (n = 7). (D) Representative traces of diaphragmatic electromyography (EMGdia) in isoflurane-anesthetized animals. (E) Quantification of EMGdia. (F) Relation between inspiratory course and integrated diaphragm amplitude with the 95% confidence ellipse. *P < 0.001, vs. injured side (paired t-test). PI: Post-injury.

Effects of C2 spinal cord hemisection on hemodynamic parameters

Immediately following C2 spinal cord hemisection, the MAP significantly decreased (before injury vs. 20 s PI, P < 0.001; **Figure 4A** and **B**). This decreased MAP was maintained at 1 hour PI (1 h PI vs. before injury, P = 0.002, and 1 h PI vs. 20 s PI, P = 0.09). At 7 days PI, the MAP returned to pre-injury values, i.e., those of the before injury (P = 0.424) and 7 d sham (P = 0.599) groups (**Figure 4B** and **C**). No significant variation in the heart rate was observed following injury (**Table 2**).

Table 2 | **Heart rate (beats/min) in anesthetized control, 20 s PI, 1 h PI, 7 d sham and 7 d PI rats**

	Mean ± SD (minimum–maximum)				
Parameters	**Control (n = 8)**	**20 s PI (n = 8)**	**1 h PI (n = 8)**	**7 d Sham (n = 9)**	**7 d PI (n = 8)**
Heart rate (beats/min)	448 ± 26 (411–478)	425 ± 30 (369–458)	439 ± 22 (406–469)	416 ± 41 (375–503)	420 ± 36 (347–465)

PI: Post-injury.

Effects of C2 spinal cord hemisection on renal function

Renal function, which relies on the MAP, was evaluated following C2 SCI. There were no differences between the control, 7 d sham, and 7 d PI groups. No difference in the glomerular filtration rate, renal threshold for glucose, and water reabsorption was observed following C2HS at 7 days PI (**Table 3**).

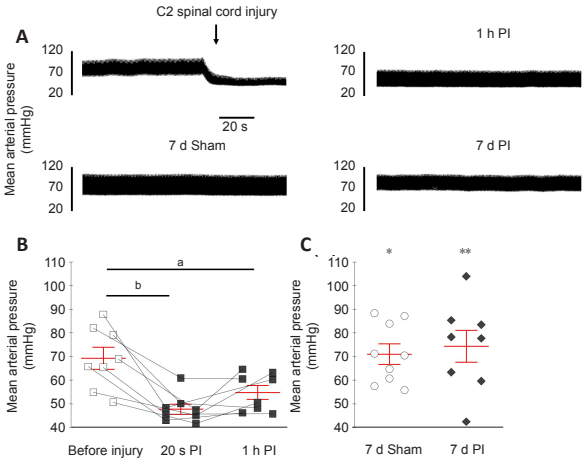

Figure 4 | **Mean arterial pressure evaluation following C2 spinal cord hemisection.** (A) Representative traces of mean arterial pressure before, during, immediately after C2 spinal cord hemisection, 1 hour PI and 7 days post-surgery (sham and 7 d PI groups). (B) Mean arterial pressure before injury, 20 seconds and 1 hour PI (n = 8). (C) Mean arterial pressure in the 7 d sham (n = 9) and 7 d PI (n = 8) groups. One-way repeated-measures analysis of variance: [a]P = 0.002, before injury vs. 1 h PI; [b]P < 0.001, before injury vs. 20 s PI. One-way analysis of variance: *P < 0.05, 7 d sham vs. 20 s PI and 1 h PI; **P < 0.01, 7 d PI vs. 20 s PI and 1 h PI. PI: Post-injury.

Table 3 | **Renal function in anesthetized control, 7 d sham and 7 d PI rats**

	Mean ± SD (minimum–maximum)		
Parameters	**Control (n = 6)**	**7 d Sham (n = 6)**	**7 d PI (n = 5)**
GFR (mL/min)	8.88 ± 3.71 (4.24–16.65)	10.52 ± 2.10 (6.68–12.41)	7.92 ± 3.74 (4.51–12.52)
RTG (mg/mL)	5.87 ± 1.14 (4.15–7.35)	6.40 ± 0.26 (6.09–6.76)	6.96 ± 0.73 (6.12–8.06)
Water reabsorption (%)	96.27 ± 1.97 (92.67–98.98)	94.91 ± 1.34 (93.31–97.13)	94.29 ± 1.27 (92.36–95.55)

GFR: Glomerular filtration rate; RTG: renal threshold for glucose.

Effects of C2 spinal cord hemisection on cardiac function

Cardiac function was evaluated by ultrasound (**Figure 5A**) in rats in the 7 d sham and 7 d PI groups. There was no difference between the two groups in anatomical parameters, including the diastolic LV diameter (P = 0.277) (**Figure 5B**), systolic LV diameter (P = 0.074) (**Figure 5C**) and aortic diameter (**Table 4**). The rats in the 7 d PI group presented a lower LV ejection fraction compared with the 7 d sham group (P = 0.036; **Figure 5D**). The rats in the 7 d sham and 7 d PI groups showed no difference in the E/A ratio (diastolic function) (P = 0.620; **Figure 5E**), isovolumetric relaxation time (**Table 4**) and aortic velocity time integral (P = 0.186; **Figure 5F**).

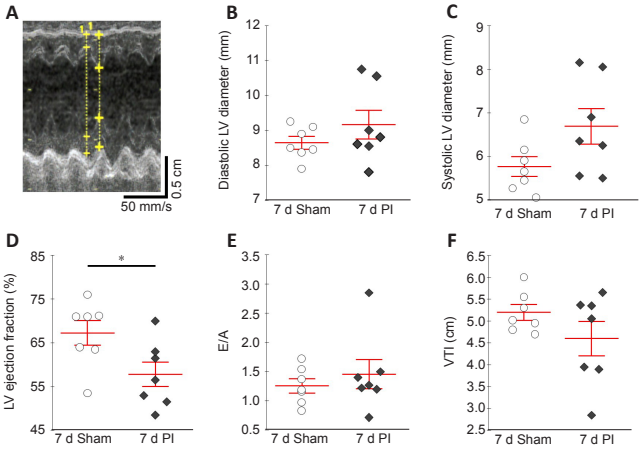

Figure 5 | **Cardiac evaluation by ultrasound 7 days post C2 spinal cord hemisection.** Evaluation of different cardiac parameters by ultrasound at 7 days post-surgery for rats in the sham (7 d sham) (n = 7) and injured (7d PI) (n = 7) groups. (A) Representative traces showing left ventricular (LV) ejection fraction during successive heart contraction cycles. The dotplots show end diastolic (B) and end systolic (C) LV diameter, LV ejection fraction (D), E/A ratio (E) and aortic velocity time integral (VTI) (F). *P = 0.036, 7 d sham vs. 7 d PI (two-tailed unpaired Student's t-test).

Table 4 | **Supplementary cardiac parameters at 7 days post C2 spinal cord hemisection**

	Mean ± SD (minimum–maximum)	
Parameters	**7 d Sham (*n* = 7)**	**7 d PI (*n* = 7)**
Aortic diameter (mm)	3.08 ± 0.25 (2.65–3.50)	2.83 ± 0.23 (2.60–3.30)
Isovolumetric relaxation time (ms)	27.5 ± 4.5 (20.5–35.1)	28.9 ± 5.8 (19.7–37.6)

Discussion

To date, this study is the first to analyze several vital physiological parameters (respiratory and cardiovascular functions and renal filtration) following a cervical C2 partial injury in rats. Surprisingly, at 7 days post-C2HS, the rats did not show any respiratory deficit under quiet breathing conditions when the respiratory parameters were evaluated by plethysmography. Several studies using the same rat model with a similar extent of injury showed an initial decrease in VT and VM associated with an increase in the respiratory frequency (Golder et al., 2001b; Lovett-Barr et al., 2012; Navarrete-Opazo et al., 2017) and progressive spontaneous restauration of these parameters over time (Navarrete-Opazo et al., 2017). This discrepancy can be explained by the development of compensatory mechanisms involving respiratory-related muscles not directly impacted by the initial injury (i.e., intercostal and abdominal muscles) (Katagiri et al., 1994). Following such an injury, in the resting state under eupneic conditions, these animals can fully maintain respiratory gas exchange homeostasis and respiratory function similar to those of pre-injury animals (Beth Zimmer et al., 2015; Navarrete-Opazo et al., 2015), leading to our observations in the injured rats. Interestingly, in the present study, despite the lack of a deficit according to plethysmography, the diaphragm activity measured by ultrasound (diaphragm displacement) and direct electromyography on the muscle (EMGdia) revealed diaphragm hemiparalysis on the injured side. Both the ultrasound and electromyography evaluations were realized on the same animals and presented a positive relationship, demonstrating the reliability of these evaluations. Respiratory deficits after cervical partial injury have been well described in many studies, mostly using invasive methods such as diaphragm electromyography using telemetry (Navarrete-Opazo et al., 2017; Bezdudnaya et al., 2018; Urban et al., 2019; Rana et al., 2021), terminal diaphragmatic recordings (Goshgarian, 1979; Vinit et al., 2006; Keomani et al., 2014; Mantilla et al., 2017; Bezdudnaya et al., 2018; Cheng et al., 2021a, b), and even terminal phrenic nerve recordings (Fuller et al., 2003; Vinit and Kastner, 2009; Lovett-Barr et al., 2012; Lee et al., 2015). However, this diaphragmatic deficit can be fully investigated in a non-invasive way, i.e., by ultrasound, resulting in a robust correlation with invasive diaphragmatic EMG activities. This correlation between diaphragmatic EMG activities and respiratory ultrasound parameters has been previously described in naïve rats (Fayssoil et al., 2021), and these data confirm the growing interest in using this non-invasive evaluation to monitor spontaneous respiratory reorganization following C2 injury in individual animals over time.

The C2HS that we performed was a complete hemisection, which impacted the bulbospinal respiratory pathway and part of the cardiovascular descending pathway (particularly, the sympathetic part; **Additional Figure 1**). Immediately after C2HS, an abrupt reduction of the MAP was observed due to the transection of half of the sympathetic innervation responsible for maintaining blood pressure homeostasis. However, this reduction was not permanent, since the MAP returned to pre-injury values by 7 days PI This result has previously been observed in several publications using similar injury models but has never been further explored. Cardiovascular parameters were used in these previous studies as a control for analyzing respiratory parameters between animal groups but were not the main research focus (Lee et al., 2016; Vinit et al., 2016; Lee and Gonzalez-Rothi, 2017). However, following total transection or contusion at the cervical or thoracic level, the MAP remains low after several weeks PI (DeVeau et al., 2017; Lujan et al., 2018; Squair et al., 2018b; Lujan and DiCarlo, 2020). In this study, the spontaneous recovery of the MAP could have been due to vascular compensation (i.e., vascular vasoconstriction) that occurred between the moment of trauma and 7 days PI by, for instance, reorganization of the sympathetic neural rewiring (i.e., around preganglionic neurons) (Krassioukov and Weaver, 1996). This neural plasticity could be sustained by oversensitization or an increase in α1-adrenergic receptor expression following spinal cord injury, as observed in preclinical rat models of complete or severe SCI (Lee et al., 2016) and patients with SCI (Davies et al., 1982). Unfortunately, we cannot confirm this hypothesis since the α1-adrenergic receptor antibodies available on the market do not produce convincing and specific labeling of these receptors in immunohistochemistry and western blot analyses (Jensen et al., 2009). We also cannot exclude that the spared fibers could be involved in the spontaneous recovery of the MAP observed overtime following C2 spinal cord hemisection. Another possibility is suggested by an analysis of raw cardiovascular parameter values. The aortic velocity time integral (**Figure 4**), heart rate (**Table 2**), and aortic diameter (**Table 4**) were not modulated by C2HS in our model. Thus, blood flow ($((d/2)^2 \times \pi \times VTI \times$ heart rate) did not appear to be impacted in this model at 7 days PI (data not shown), leading to the recovery of the pre-injury MAP. Interestingly, no significant variation in the heart rate after injury was observed, as reported in previous studies of C2HS animals (Golder et al., 2001a; Lee et al., 2013, 2014; Lee and Gonzalez-Rothi, 2017). This could be partially because the vagus nerve, which is known to mediate the heartbeat rhythmicity (Golder et al., 2001b), is not directly impacted by C2 SCI, and the sympathetic inputs were only partly impacted by the partial spinal injury that spared some sympathetic fibers. However, in models of complete or severe SCI, a reduced heart rate is observed up to 2 weeks PI (Mayorov et al., 2001; Lujan et al., 2018). More in-depth studies are needed to confirm these hypotheses.

Blood pressure is directly linked to renal function, and blood pressure function and homeostasis are dependent on renal blood flow. A low cardiac output or MAP can damage the kidneys (Langenberg et al., 2005; Badin et al., 2011), and a disruption of the renal sympathetic output can as well as induce renal dysfunction (Sweis and Biller, 2017); however, the renal function evaluation in our C2HS rats at 7 days PI showed no modification of any parameters studied, which was unsurprising, given that the MAP was restored to pre-injury values by this timepoint. Nevertheless, we cannot rule out that immediately after injury, our rats may have presented a reduced MAP that could have caused transient renal dysfunction (Rodríguez-Romero et al., 2018).

Even though spontaneous recovery of the MAP was observed over time after C2HS injury in rats, cardiac function evaluation by ultrasound at 7 days PI revealed remnant systolic dysfunction characterized by a reduced LV ejection fraction in our study. However, no other cardiac parameters (i.e., anatomy and diastolic function) differed from those of the Sham rats. Interestingly, studies depicting cardiac dysfunction often use animals spinally contused at the thoracic level. In a rat model of T2 contusion, reductions in the stroke volume, end-diastolic volume, and cardiac output or LV internal diameter during diastole were observed at 7 days PI, in addition to a reduced LV ejection fraction (DeVeau et al., 2018; Squair et al., 2018b). These deficits persisted at least until 5–6 weeks PI (DeVeau et al., 2018; Squair et al., 2018b). In contrast, no changes in the LV ejection fraction were found at 5 weeks PI following a T3 moderate or severe contusion compared to a T2 contusion (Squair et al., 2018a). The severe T3 contusion led to a reduced stroke volume, LV internal diameter during diastole, systolic volume, and end-systolic volume (Squair et al., 2018a). Several sympathetic descending fibers could remain partially intact after a severe contusion injury, and these residual fibers cannot fully sustain the sympathetic output, leading to heart dysfunction. In the present study, even though half of the descending sympathetic fibers remained intact on the contralateral side after C2HS (**Figure 2**), the remaining innervation of these sympathetic fibers was not sufficient to maintain a normal LV ejection fraction at 7 days PI but was adequate to avoid other cardiac dysfunctions, such as those found in thoracic contusion or transection models (Poormasjedi-Meibod et al., 2019). A reduced LV ejection fraction is likely to occur acutely after hemisection and could be the cause of the post-injury MAP decrease in this study. However, even when MAP recovery spontaneously occurs over time by some compensatory mechanism at 7 days PI, such as compensatory vascular vasoconstriction, the systolic deficit persists. More studies are needed to determine the mechanisms underlying this spontaneous MAP recovery and the putative sympathetic intraspinal neuronal rewiring following C2HS.

This study however had some limitations. We were not able to evaluate the cardiac function immediately following the spinal cord injury due to experimental and technical feasibility. Although we observe a cardiac systolic dysfunction at 7 days PI, we only hypothesize the C2HS induced it right after injury. We also did not reveal the potential mechanism responsible for the compensation in MAP observed at 7 days PI. Further investigation will be required to elucidate the specific mechanisms involved in this phenomenon.

In conclusion, this study demonstrated that C2HS in a rat model leads to diverse vital pathophysiological defects that can, in some cases, undergo spontaneous restoration. A better broad characterization of the physiopathology of high SCI would benefit the understanding of evaluations of putative therapeutics to further increase observed cardiorespiratory recovery.

Acknowledgments: *We thank Valentin Vanhée (Université Paris-Saclay) for his assistance in revising this manuscript. The authors thank the Radiology Department of Raymond Poincaré hospital (AP-HP) for letting us utilize the ultrasound equipment.*
Author contributions: *Investigation, formal analysis, visualization, writing - original draft, review & editing: PMF. Investigation, methodology, review & editing: AM. Conceptualization, investigation, methodology, supervision, funding acquisition, writing - review & editing: AF. Conceptualization, methodology, investigation, supervision, project administration, funding acquisition, writing - review & editing: SV. All authors approved the final version of the paper.*
Conflicts of interest: *There are no conflicts of interest.*
Editor note: SV is an Editorial Board member of Neural Regeneration Research. He was blinded from reviewing or making decisions on the manuscript. The article was subject to the journal's standard procedures, with peer review handled independently of this Editorial Board member and their research groups.
Availability of data and materials: *All data generated or analyzed during this study are included in this published article and its supplementary information files.*

Additional file:

Additional Figure 1: *Schematic of the impact of C2 cervical spinal cord injuries on respiratory and cardiovascular descending pathways.*

References

Ahuja CS, Wilson JR, Nori S, Kotter MRN, Druschel C, Curt A, Fehlings MG (2017) Traumatic spinal cord injury. Nat Rev Dis Primers 3:17018.

Badin J, Boulain T, Ehrmann S, Skarzynski M, Bretagnol A, Buret J, Benzekri-Lefevre D, Mercier E, Runge I, Garot D, Mathonnet A, Dequin PF, Perrotin D (2011) Relation between mean arterial pressure and renal function in the early phase of shock: a prospective, explorative cohort study. Crit Care 15:R135.

Behan M, Kinkead R (2011) Neuronal control of breathing: sex and stress hormones. Compr Physiol 1:2101-2139.

Beth Zimmer M, Grant JS, Ayar AE, Goshgarian HG (2015) Ipsilateral inspiratory intercostal muscle activity after C2 spinal cord hemisection in rats. J Spinal Cord Med 38:224-230.

Bezdudnaya T, Hormigo KM, Marchenko V, Lane MA (2018) Spontaneous respiratory plasticity following unilateral high cervical spinal cord injury in behaving rats. Exp Neurol 305:56-65.

Biering-Sørensen F, Biering-Sørensen T, Liu N, Malmqvist L, Wecht JM, Krassioukov A (2018) Alterations in cardiac autonomic control in spinal cord injury. Auton Neurosci 209:4-18.

Bravo G, Hong E, Rojas G, Guízar-Sahagún G (2002) Sympathetic blockade significantly improves cardiovascular alterations immediately after spinal cord injury in rats. Neurosci Lett 319:95-98.

Chay W, Kirshblum S (2020) Predicting outcomes after spinal cord injury. Phys Med Rehabil Clin N Am 31:331-343.

Cheng L, Sami A, Ghosh B, Goudsward HJ, Smith GM, Wright MC, Li S, Lepore AC (2021a) Respiratory axon regeneration in the chronically injured spinal cord. Neurobiol Dis 155:105389.

Cheng L, Sami A, Ghosh B, Urban MW, Heinsinger NM, Liang SS, Smith GM, Wright MC, Li S, Lepore AC (2021b) LAR inhibitory peptide promotes recovery of diaphragm function and multiple forms of respiratory neural circuit plasticity after cervical spinal cord injury. Neurobiol Dis 147:105153.

Davies B, Sudera D, Sagnella G, Marchesi-Saviotti E, Mathias C, Bannister R, Sever P (1982) Increased numbers of alpha receptors in sympathetic denervation supersensitivity in man. J Clin Investig 69:779-784.

DeVeau KM, Harman KA, Squair JW, Krassioukov AV, Magnuson DSK, West CR (2017) A comparison of passive hindlimb cycling and active upper-limb exercise provides new insights into systolic dysfunction after spinal cord injury. Am J Physiol Heart Circ Physiol 313:H861-870.

DeVeau KM, Martin EK, King NT, Shum-Siu A, Keller BB, West CR, Magnuson DSK (2018) Challenging cardiac function post-spinal cord injury with dobutamine. Auton Neurosci 209:19-24.

Ditterline BL, Wade S, Ugiliweneza B, Singam NSV, Harkema SJ, Stoddard MF, Hirsch GA (2020) Systolic and diastolic function in chronic spinal cord injury. PLoS One 15:e0236490.

Driussi C, Ius A, Bizzarini E, Antonini-Canterin F, d'Andrea A, Bossone E, Vriz O (2014) Structural and functional left ventricular impairment in subjects with chronic spinal cord injury and no overt cardiovascular disease. J Spinal Cord Med 37:85-92.

Eckert MJ, Martin MJ (2017) Trauma: spinal cord injury. Surg Clin North Am 97:1031-1045.

Eli I, Lerner DP, Ghogawala Z (2021) Acute traumatic spinal cord injury. Neurol Clin 39:471-488.

Fayssoil A, Michel-Flutot P, Lofaso F, Carlier R, El Hajjam M, Vinit S, Mansart A (2021) Analysis of inspiratory and expiratory muscles using ultrasound in rats: A reproducible and non-invasive tool to study respiratory function. Respir Physiol Neurobiol 285:103596.

Fayssoil A, Behin A, Ogna A, Mompoint D, Amthor H, Clair B, Laforet P, Mansart A, Prigent H, Orlikowski D, Stojkovic T, Vinit S, Carlier R, Eymard B, Lofaso F, Annane D (2018) Diaphragm: pathophysiology and ultrasound imaging in neuromuscular disorders. J Neuromuscul Dis 5:1-10.

Feldman JL, Loewy AD, Speck DF (1985) Projections from the ventral respiratory group to phrenic and intercostal motoneurons in cat: an autoradiographic study. J Neurosci 5:1993-2000.

Feldman JL, Del Negro CA, Gray PA (2013) Understanding the rhythm of breathing: so near, yet so far. Annu Rev Physiol 75:423-452.

Fuller DD, Johnson SM, Olson EB, Jr., Mitchell GS (2003) Synaptic pathways to phrenic motoneurons are enhanced by chronic intermittent hypoxia after cervical spinal cord injury. J Neurosci 23:2993-3000.

Fuller DD, Doperalski NJ, Dougherty BJ, Sandhu MS, Bolser DC, Reier PJ (2008) Modest spontaneous recovery of ventilation following chronic high cervical hemisection in rats. Exp Neurol 211:97-106.

Ghali MGZ (2017) The crossed phrenic phenomenon. Neural Regen Res 12:845-864.

Golder FJ, Reier PJ, Bolser DC (2001a) Altered respiratory motor drive after spinal cord injury: Supraspinal and bilateral effects of a unilateral lesion. J Neurosci 21:8680-8689.

Golder FJ, Reier PJ, Davenport PW, Bolser DC (2001b) Cervical spinal cord injury alters the pattern of breathing in anesthetized rats. J Appl Physiol 91:2451-2458.

Goshgarian HG (1979) Developmental plasticity in the respiratory pathway of the adult rat. Exp Neurol 66:547-555.

Goshgarian HG (2003) The crossed phrenic phenomenon: a model for plasticity in the respiratory pathways following spinal cord injury. J Appl Physiol (1985) 94:795-810.

Harman KA, States G, Wade A, Stepp C, Wainwright G, DeVeau K, King N, Shum-Siu A, Magnuson DSK (2018) Temporal analysis of cardiovascular control and function following incomplete T3 and T10 spinal cord injury in rodents. Physiol Rep 6:e13634.

Hou S, Rabchevsky AG (2014) Autonomic consequences of spinal cord injury. Compr Physiol 4:1419-1453.

Ioannis T, George S, Nikolaos K, George M, Charalampos P, Nikolaos D, Spyridon S, Michael S (2016) Evaluation of diaphragmatic mobility following intra-abdominal sub-diaphragmatic fixation of a double-layered mesh in rats. Acta Cir Bras 31:235-242.

Jensen BC, Swigart PM, Simpson PC (2009) Ten commercial antibodies for alpha-1-adrenergic receptor subtypes are nonspecific. Naunyn Schmiedebergs Arch Pharmacol 379:409-412.

Jesus I, Michel-Flutot P, Deramaudt TB, Paucard A, Vanhee V, Vinit S, Bonay M (2021) Effects of aerobic exercise training on muscle plasticity in a mouse model of cervical spinal cord injury. Sci Rep 11:112.

Katagiri M, Young RN, Platt RS, Kieser TM, Easton PA (1994) Respiratory muscle compensation for unilateral or bilateral hemidiaphragm paralysis in awake canines. J Appl Physiol 77:1972-1982.

Keomani E, Deramaudt TB, Petitjean M, Bonay M, Lofaso F, Vinit S (2014) A murine model of cervical spinal cord injury to study post-lesional respiratory neuroplasticity. J Vis Exp 87:e51235.

Kessler KM, Pina I, Green B, Burnett B, Laighold M, Bilsker M, Palomo AR, Myerburg RJ (1986) Cardiovascular findings in quadriplegic and paraplegic patients and in normal subjects. Am J Cardiol 58:525-530.

Krassioukov A, Claydon VE (2006) The clinical problems in cardiovascular control following spinal cord injury: an overview. Prog Brain Res 152:223-229.

Krassioukov AV, Weaver LC (1996) Morphological changes in sympathetic preganglionic neurons after spinal cord injury in rats. Neuroscience 70:211-225.

Langenberg C, Bellomo R, May C, Wan L, Egi M, Morgera S (2005) Renal blood flow in sepsis. Crit Care 9:R363-374.

Lee JS, Fang SY, Roan JN, Jou IM, Lam CF (2016) Spinal cord injury enhances arterial expression and reactivity of α1-adrenergic receptors-mechanistic investigation into autonomic dysreflexia. Spine J 16:65-71.

Lee KZ, Dougherty BJ, Sandhu MS, Lane MA, Reier PJ, Fuller DD (2013) Phrenic motoneuron discharge patterns following chronic cervical spinal cord injury. Exp Neurol 249:20-32.

Lee KZ, Huang YJ, Tsai IL (2014) Respiratory motor outputs following unilateral midcervical spinal cord injury in the adult rat. J Appl Physiol 116:395-405.

Lee KZ, Sandhu MS, Dougherty BJ, Reier PJ, Fuller DD (2015) Hypoxia triggers short term potentiation of phrenic motoneuron discharge after chronic cervical spinal cord injury. Exp Neurol 263:314-324.

Lee KZ, Gonzalez-Rothi EJ (2017) Contribution of 5-HT2A receptors on diaphragmatic recovery after chronic cervical spinal cord injury. Respir Physiol Neurobiol 244:51-55.

Liang Y, Arakawa K, Ueta K, Matsushita Y, Kuriyama C, Martin T, Du F, Liu Y, Xu J, Conway B, Conway J, Polidori D, Ways K, Demarest K (2012) Effect of canagliflozin on renal threshold for glucose, glycemia, and body weight in normal and diabetic animal models. PLoS One 7:e30555.

Lipski J, Bektas A, Porter R (1986) Short latency inputs to phrenic motoneurones from the sensorimotor cortex in the cat. Exp Brain Res 61:280-290.

Lovett-Barr MR, Satriotomo I, Muir GD, Wilkerson JE, Hoffman MS, Vinit S, Mitchell GS (2012) Repetitive intermittent hypoxia induces respiratory and somatic motor recovery after chronic cervical spinal injury. J Neurosci 32:3591-3600.

Lujan HL, DiCarlo SE (2020) Direct comparison of cervical and high thoracic spinal cord injury reveals distinct autonomic and cardiovascular consequences. J Appl Physiol 128:554-564.

Lujan HL, Tonson A, Wiseman RW, DiCarlo SE (2018) Chronic, complete cervical(6-7) cord transection: distinct autonomic and cardiac deficits. J Appl Physiol 124:1471-1482.

Mantilla CB, Gransee HM, Zhan WZ, Sieck GC (2017) Impact of glutamatergic and serotonergic neurotransmission on diaphragm muscle activity after cervical spinal hemisection. J Neurophysiol 118:1732-1738.

Matamis D, Soilemezi E, Tsagourias M, Akoumianaki E, Dimassi S, Boroli F, Richard J-CM, Brochard L (2013) Sonographic evaluation of the diaphragm in critically ill patients. Technique and clinical applications. Intensive Care Med 39:801-810.

Mayorov DN, Adams MA, Krassioukov AV (2001) Telemetric blood pressure monitoring in conscious rats before and after compression injury of spinal cord. J Neurotrauma 18:727-736.

Michel-Flutot P, Mansart A, Deramaudt TB, Jesus I, Lee KZ, Bonay M, Vinit S (2021) Permanent diaphragmatic deficits and spontaneous respiratory plasticity in a mouse model of incomplete cervical spinal cord injury. Respir Physiol Neurobiol 284:103568.

Michel-Flutot P, Jesus I, Vanhee V, Bourcier CH, Emam L, Ouguerroudj A, Lee KZ, Zholudeva LV, Lane MA, Mansart A, Bonay M, Vinit S (2022) Effects of chronic high-frequency rTMS protocol on respiratory neuroplasticity following C2 spinal cord hemisection in rats. Biology (Basel) 11:473.

Moreira RS, Irigoyen M, Sanches TR, Volpini RA, Camara NO, Malheiros DM, Shimizu MH, Seguro AC, Andrade L (2014) Apolipoprotein A-I mimetic peptide 4F attenuates kidney injury, heart injury, and endothelial dysfunction in sepsis. Am J Physiol Regul Integr Comp Physiol 307:R514-524.

Navarrete-Opazo A, Vinit S, Dougherty BJ, Mitchell GS (2015) Daily acute intermittent hypoxia elicits functional recovery of diaphragm and inspiratory intercostal muscle activity after acute cervical spinal injury. Exp Neurol 266:1-10.

Navarrete-Opazo A, Dougherty BJ, Mitchell GS (2017) Enhanced recovery of breathing capacity from combined adenosine 2A receptor inhibition and daily acute intermittent hypoxia after chronic cervical spinal injury. Exp Neurol 287:93-101.

Pacher P, Nagayama T, Mukhopadhyay P, Bátkai S, Kass DA (2008) Measurement of cardiac function using pressure-volume conductance catheter technique in mice and rats. Nat Protoc 3:1422-1434.

Papadimitriou L, Georgiopoulou VV, Kort S, Butler J, Kalogeropoulos AP (2016) Echocardiography in acute heart failure: current perspectives. J Card Fail 22:82-94.

Poormasjedi-Meibod MS, Mansouri M, Fossey M, Squair JW, Liu J, McNeill JH, West CR (2019) Experimental spinal cord injury causes left-ventricular atrophy and is associated with an upregulation of proteolytic pathways. J Neurotrauma 36:950-961.

Rana S, Sunshine MD, Greer JJ, Fuller DD (2021) Ampakines stimulate diaphragm activity after spinal cord injury. J Neurotrauma 38:3467-3482.

Rodríguez-Romero V, Guízar-Sahagún G, Castañeda-Hernández G, Reyes JL, Cruz-Antonio L (2018) Early systemic alterations in severe spinal cord injury: an experimental study on the impact of injury level on renal function. Spine 43:E885-890.

Schneider CA, Rasband WS, Eliceiri KW (2012) NIH Image to ImageJ: 25 years of image analysis. Nat Methods 9:671-675.

Shimron M, Williams L, Hazanov Y, Ghanim D, Kinany W, Amir O, Carasso S (2018) Clinical and echocardiographic characteristics of patients in sinus rhythm, normal left ventricular function, and indeterminate diastolic function. Echocardiography 35:792-797.

Smith GL, Lichtman JH, Bracken MB, Shlipak MG, Phillips CO, DiCapua P, Krumholz HM (2006) Renal impairment and outcomes in heart failure: systematic review and meta-analysis. J Am Coll Cardiol 47:1987-1996.

Squair JW, Liu J, Tetzlaff W, Krassioukov AV, West CR (2018a) Spinal cord injury-induced cardiomyocyte atrophy and impaired cardiac function are severity dependent. Exp Physiol 103:179-189.

Squair JW, West CR, Popok D, Assinck P, Liu J, Tetzlaff W, Krassioukov AV (2017) High thoracic contusion model for the investigation of cardiovascular function after spinal cord injury. J Neurotrauma 34:671-684.

Squair JW, DeVeau KM, Harman KA, Poormasjedi-Meibod MS, Hayes B, Liu J, Magnuson DSK, Krassioukov AV, West CR (2018b) Spinal cord injury causes systolic dysfunction and cardiomyocyte atrophy. J Neurotrauma 35:424-434.

Sweis R, Biller J (2017) Systemic complications of spinal cord injury. Curr Neurol Neurosci Rep 17:8.

Terada J, Mitchell GS (2011) Diaphragm long-term facilitation following acute intermittent hypoxia during wakefulness and sleep. J Appl Physiol 110:1299-1310.

Urban MW, Ghosh B, Block CG, Strojny LR, Charsar BA, Goulão M, Komaravolu SS, Smith GM, Wright MC, Li S, Lepore AC (2019) Long-distance axon regeneration promotes recovery of diaphragmatic respiratory function after spinal cord injury. eNeuro 6:ENEURO.0096-19.2019.

Vandeweerd JM, Hontoir F, De Knoop A, De Swert K, Nicaise C (2018) Retrograde neuroanatomical tracing of phrenic motor neurons in mice. J Vis Exp:56758.

Vinit S, Gauthier P, Stamegna JC, Kastner A (2006) High cervical lateral spinal cord injury results in long-term ipsilateral hemidiaphragm paralysis. J Neurotrauma 23:1137-1146.

Vinit S, Kastner A (2009) Descending bulbospinal pathways and recovery of respiratory motor function following spinal cord injury. Respir Physiol Neurobiol 169:115-122.

Vinit S, Keomani E, Deramaudt TB, Bonay M, Petitjean M (2016) Reorganization of respiratory descending pathways following cervical spinal partial section investigated by transcranial magnetic stimulation in the rat. PLoS One 11:e0148180.

Warren PM, Steiger SC, Dick TE, MacFarlane PM, Alilain WJ, Silver J (2018) Rapid and robust restoration of breathing long after spinal cord injury. Nat Commun 9:4843-4843.

Weaver LC, Cassam AK, Krassioukov AV, Llewellyn-Smith IJ (1997) Changes in immunoreactivity for growth associated protein-43 suggest reorganization of synapses on spinal sympathetic neurons after cord transection. Neuroscience 81:535-551.

West CR, Mills P, Krassioukov AV (2012) Influence of the neurological level of spinal cord injury on cardiovascular outcomes in humans: a meta-analysis. Spinal Cord 50:484-492.

Zhu Z, Li J, Yang D, Gao F, Du L, Yang M (2021) Ultrasonographic evaluation of diaphragm thickness and excursion in patients with cervical spinal cord injury. J Spinal Cord Med 44:742-747.

C-Editors: Zhao M, Liu WJ; S-Editor: Li CH; L-Editors: Li CH, Song LP; T-Editor: Jia Y

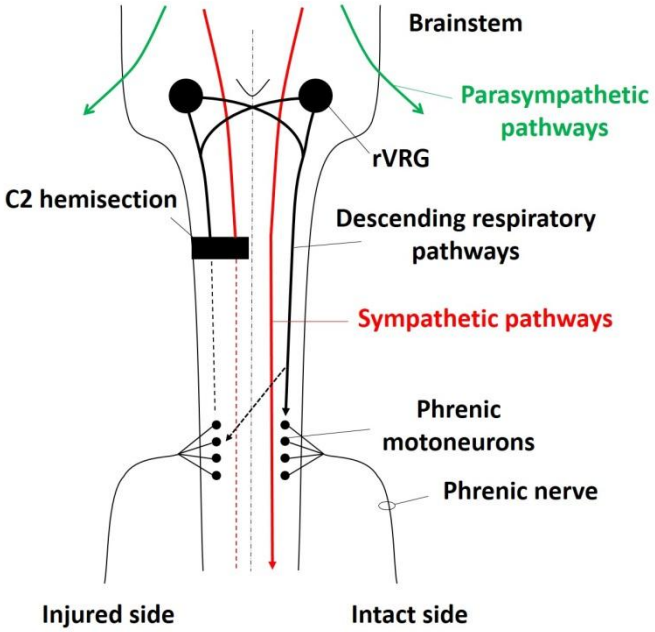

Additional Figure 1 Schematic of the impact of C2 cervical spinal cord injuries on respiratory and cardiovascular descending pathways.

Schematic representing the impact of a C2 spinal cord hemisection on the respiratory descending pathways (black arrow), the parasympathetic descending pathways (green arrow) and the sympathetic descending pathways (red arrow). The C2 hemisection induces an interruption of the descending pathways below the injured site for the descending respiratory (black dotted line) and sympathetic (red dotted line) pathways. rVRG: Rostral ventral respiratory group.